On the Abruptness of Bølling–Allerød Warming

ZHAN SU AND ANDREW P. INGERSOLL

Division of Geological and Planetary Sciences, California Institute of Technology, Pasadena, California

FENG HE

Center for Climatic Research, Nelson Institute for Environmental Studies, University of Wisconsin–Madison, Madison, Wisconsin, and College of Earth, Ocean, and Atmospheric Sciences, Oregon State University, Corvallis, Oregon

(Manuscript received 23 September 2015, in final form 30 March 2016)

ABSTRACT

Previous observations and simulations suggest that an approximate 3°–5°C warming occurred at intermediate depths in the North Atlantic over several millennia during Heinrich stadial 1 (HS1), which induces warm salty water (WSW) lying beneath surface cold freshwater. This arrangement eventually generates ocean convective available potential energy (OCAPE), the maximum potential energy releasable by adiabatic vertical parcel rearrangements in an ocean column. The authors find that basin-scale OCAPE starts to appear in the North Atlantic (~67.5°–73.5°N) and builds up over decades at the end of HS1 with a magnitude of about 0.05 J kg^{-1}. OCAPE provides a key kinetic energy source for thermobaric cabbeling convection (TCC). Using a high-resolution TCC-resolved regional model, it is found that this decadal-scale accumulation of OCAPE ultimately overshoots its intrinsic threshold and is released abruptly (~1 month) into kinetic energy of TCC, with further intensification from cabbeling. TCC has convective plumes with approximately 0.2–1-km horizontal scales and large vertical displacements (~1 km), which make TCC difficult to be resolved or parameterized by current general circulation models. The simulation herein indicates that these local TCC events are spread quickly throughout the OCAPE-contained basin by internal wave perturbations. Their convective plumes have large vertical velocities (~8–15 cm s^{-1}) and bring the WSW to the surface, causing an approximate 2°C sea surface warming for the whole basin (~700 km) within a month. This exposes a huge heat reservoir to the atmosphere, which helps to explain the abrupt Bølling–Allerød warming.

1. Introduction

In the last deglaciation, the North Atlantic region experienced notable surface cooling during Heinrich stadial 1 [HS1, ~17 ka (1 ka = 1000 years ago); Clark et al. 2002; Hemming 2004]. Potential surface meltwater discharge to the North Atlantic, as assumed in numerous studies (Broecker 1994; Ganopolski and Rahmstorf 2001; Buizert et al. 2014; Carlson and Clark 2012), may contribute to this cooling. The cooling is followed by an abrupt (years to decades) surface warming at the end of HS1, that is, at the onset of the Bølling–Allerød (BA) warming (~14.5 ka) (McManus et al. 2004; Alley 2007). This abrupt warming is one of the Dansgaard–Oeschger (D–O) warm events (i.e., the warming phase of D–O events). As reviewed by Rahmstorf 2002, there are many mechanisms proposed to explain the D–O events. (e.g., Liu et al. 2009; Weaver et al. 2003; Knorr and Lohmann 2007; Ganopolski and Rahmstorf 2001). With exceptions (e.g., Clement and Cane 1999), most mechanisms are closely related to the Atlantic meridional overturning circulation (AMOC) such as the idea of "thermohaline circulation bistability" (Broecker et al. 1985) and "salt oscillator" (Broecker et al. 1990). Ganopolski and Rahmstorf (2001, 2002) propose a mechanism associated with the stability of AMOC and stochastic resonance, which explains many key observed features of D–O events, including the three-phase time evolution, spatial pattern, and hemispheric seesaw. In this paper, we focus on the mechanism for explaining the abruptness of the D–O surface warm events (e.g., the abrupt BA warming during the transition from HS1 to BA). This has not received as much attention as the cooling in the North Atlantic induced by, for example, the shutdown of the AMOC.

Many previous studies for the D–O warm events involve an established convective-threshold mechanism

Corresponding author address: Zhan Su, Division of Geological and Planetary Sciences, California Institute of Technology, Pasadena, CA 91125.
E-mail: zssu@caltech.edu

DOI: 10.1175/JCLI-D-15-0675.1

(e.g., Ganopolski and Rahmstorf 2001; Winton 1995; Rasmussen and Thomsen 2004; Winton and Sarachik 1993): the cold freshwater (CFW) typically overlies the warm salty water (WSW) in the North Atlantic after Heinrich events, where the WSW gradually warms up (as detailed below). This warming of intermediate-depth WSW and the potential reduction of surface freshwater supply reduce the static stability of the ocean until the threshold of static instability is exceeded in the North Atlantic. Then the convection renews and brings the WSW upward. This rapidly releases a large amount of stored potential energy of heat to the surface and invigorates the AMOC. Therefore this convective-threshold mechanism may explain the abrupt D–O warm events. Rahmstorf (2001) has investigated the threshold onset of convection (for CFW overlying WSW) and its bistable nature, which could strongly modulate the AMOC and the climate of the North Atlantic (see also Rahmstorf 1994, 1995a,b).

In this study we propose a modified convective-threshold mechanism as an amendment to the above established convective-threshold mechanism. The main difference is as follows. In the modified mechanism, convection occurs due to thermobaric instability, which occurs before static instability (the established mechanism) is reached. In other words, the convection that truly occurs in the BA warming may be due to the thermobaric instability rather than the static instability. In contrast to the static instability, thermobaric instability is a different type of fluid instability (Ingersoll 2005). It not only releases the stored heat of WSW, but also releases the ocean convective available potential energy (OCAPE) into kinetic energy of the convection. Further, it typically induces a much more abrupt (shorter time scale) ocean overturning (vertical mixing) and typically reaches deeper depths than static instability in convection events (Denbo and Skyllingstad 1996; Akitomo 1999). Finally, it may provide an intrinsic/self-consistent component for the climate system. This is because it relies on the heat/salt transport of the global ocean circulation, rather than an essentially "arbitrary" surface freshwater forcing assumed in numerous studies (see section 4 for more discussion). However, whether it substantially changes the evolution of the BA warming is less clear. It is possible that both the modified and the established convective-threshold mechanisms, if they can both occur, would eventually lead to a similar final overturning state of the North Atlantic after years or decades, although what truly occurs may be the modified mechanism rather than the established mechanism as mentioned above.

Although the surface freshwater forcing may make a contribution, both the modified and the established convective-threshold mechanisms are associated with the observed millennial-scale (~3°–5°C) warming at intermediate depths (~1–2-km depths) of the North Atlantic during HS1 (Thiagarajan et al. 2014; Marcott et al. 2011; Alvarez-Solas et al. 2010). The induced intermediate-depth ocean is about 4°C warmer than the shallower water above [Thiagarajan et al. 2014; see similar observations in Rasmussen et al. (2003), Rasmussen and Thomsen (2004), and Dokken and Jansen (1999)]. Many numerical simulations also indicate similar millennial-scale warming (~2°–9°C) at intermediate depths of North Atlantic, as a response to the largely reduced AMOC during stadials (Shaffer et al. 2004; Stouffer et al. 2006; Clark et al. 2007; Arzel et al. 2010; Brady and Otto-Bliesner 2011). For example, Fig. 1 illustrates the almost 3°C warming at around 0.3–2-km depths in the North Atlantic during HS1 (~2300-yr duration) from the Community Climate System Model, version 3 (CCSM3), simulation of the last deglaciation (Liu et al. 2009; He et al. 2013). This phenomenon may have at least two explanations: 1) Less convective heat is lost into the atmosphere from the intermediate-depth North Atlantic due to the suppressed deep convection during stadials (Knutti et al. 2004); also, 2) heat is transported from the Southern Ocean and tropical Atlantic, which may be related to the vertical heat diffusion and eddy stirrings, to the North Atlantic at intermediate depths by the subpolar gyre and the weakened AMOC during stadials (Winton 1995; Mignot et al. 2007; Shaffer et al. 2004).

In section 2, we demonstrate that millennial-scale warming at intermediate depths of the North Atlantic during HS1 could eventually generate OCAPE to a large

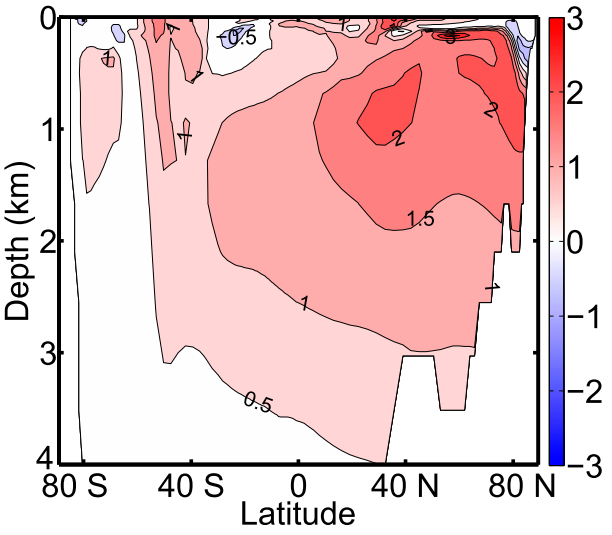

FIG. 1. The changes of Atlantic zonal mean potential temperature θ (°C) during HS1 (~2300-yr duration), from the CCSM3 simulation of the last deglaciation (Liu et al. 2009; He et al. 2013). The figure shows that the North Atlantic became warmer (~1.5°–3°C) at intermediate depths (beneath ~200-m depth) but remained unchanged or became colder at the ocean surface at 40°–80°N. This millennial-scale process generates WSW lying beneath CFW, which could accumulate OCAPE (Fig. 3).

magnitude ($\sim$0.05 J kg^{-1}). OCAPE is a vital kinetic energy source for thermobaric cabbeling convection [TCC; see TCC studies in Akitomo et al. (1995), Akitomo (1999, 2006), and Harcourt 2005)]. In section 3, we present high-resolution numerical simulations for our modified convective-threshold mechanism: We illustrate that this continual accumulation of OCAPE eventually overshoots its intrinsic threshold and causes a sudden release of OCAPE that powers dramatic TCC events. This brings warm salty water to the surface and warms the sea surface of the whole basin ($\sim$700-km scale) by about 2°C within one month. In section 4 we discuss implications.

2. Basin-scale OCAPE in the North Atlantic at the end of HS1

OCAPE is a newly developed and well-defined concept (Su et al. 2016a,b). It quantifies the maximal potential energy of an ocean column that is available to be released into kinetic energy by the transition from the current state to the minimum potential energy (PE) state through adiabatic vertical parcel rearrangements:

$$\text{OCAPE} = \text{PE(current state)} - \text{PE(minimum PE state)}. \quad (1)$$

The same energy concept, although not as formally formulated as OCAPE, was discussed in section 7 of Ingersoll (2005) and sections 2 and 3 of Adkins et al. (2005). Although OCAPE can be computed numerically for any idealized equation of state, all OCAPE values in this manuscript are computed based on the full nonlinear equation of state of seawater (Jackett et al. 2006). OCAPE typically appears in an ocean column when cold freshwater lies above warm salty water. This type of ocean column may be susceptible to TCC even if the column has a statically stable stratification. Thus TCC is not the regular surface buoyancy-driven convection. OCAPE offers a main kinetic energy source for TCC and it arises from thermobaricity—the significant increase of the thermal expansion coefficient of seawater with the depth (Fig. 2a). The appendix illustrates the mechanism for the release of OCAPE into kinetic energy during TCC events.

TCC is difficult to be directly observed due to its short time scales ($\sim$days) and severe polar observational conditions during wintertime. However, indirect observational evidences and theoretical or numerical analysis suggest that the modern Weddell Sea is susceptible to TCC (i.e., the release of OCAPE to kinetic energy) [detailed in Akitomo et al. (1995), Akitomo (1999, 2006), McPhee (2000, 2003), and Harcourt (2005)]. OCAPE exists in the modern ocean: Figs. 2c,d display a statically stable stratified profile with CFW overlying WSW that was observed in the Weddell Sea (McPhee et al. 1996). This profile contains a column-averaged OCAPE of 1.1 $\times$ 10^{-3} J kg^{-1} [equivalent to a velocity of 4.7 cm s^{-1} if converted into kinetic energy, following the scaling of velocity approximately (2 $\times$ kinetic energy/mass)$^{0.5}$]. Figures 2e–h show our simulated TCC initialized by this observed profile and triggered by realistic surface perturbations (homogeneous brine rejection equivalent to 1 cm day^{-1} sea ice formation, applied to the whole domain for the initial 4.2 days). The model is two-dimensional (vertical and horizontal) and nonhydrostatic in a rotating frame [essentially the same model of Akitomo et al. (1995) and Akitomo (2006), using the full nonlinear equation of state from Jackett et al. (2006)]. We apply a numerical resolution of 50 m in the horizontal and 10 m in the vertical, which allows the resolving of TCC (Akitomo 2006; Harcourt 2005). TCC begins after about 2 days and drives a thorough mixing within 10 days for the whole 10-km domain. The convective plumes have a horizontal scale of approximately 0.2–1 km and vertical velocities of 4–7 cm s^{-1}, which are powered by OCAPE and cabbeling effect. This result is consistent with those of Akitomo (2006), who simulates that TCC causes an approximate 1-km depth of convective overturning for an approximate 10-km horizontal-scale water column around Maud Rise of the Weddell Sea. TCC hence impacts the Weddell gyre dynamics and the production of Antarctic Bottom Water there (e.g., Su et al. 2014).

Next we demonstrate that OCAPE could exist in the North Atlantic at the end of HS1. We use the monthly output from the CCSM3 simulation of the last deglaciation (Liu et al. 2009; He et al. 2013. See Fig. 1 for its simulated intermediate-depth warming during HS1, which induces CFW overlying WSW and thus may generate OCAPE). As shown in Figs. 3a–d, we find that a basin-scale OCAPE pattern first appears in the North Atlantic ($\sim$67.5°–73.5°N) at about the end of HS1 (14.542 ka) and grows larger in both the horizontal scale ($\sim$700 km) and the magnitude ($\sim$0.05 J kg^{-1}) for a few decades until the BA warming. In detail, we show in Fig. 3c a dashed white line ($\sim$6°W and 67.5°–73.5°N; 14.536 ka) that approximately crosses the center of the OCAPE pattern. It has CFW ($\sim$0–0.5-km depths) overlying the WSW and has a statically stable stratification (Fig. 3e). Its averaged OCAPE is about 0.05 J kg^{-1}, meaning a convection velocity of approximately 30 cm s^{-1} if all OCAPE is converted into kinetic energy.

We now discuss the credibility of the build-up of OCAPE found in CCSM3 (Figs. 3a–d). (i) The OCAPE of an ocean column is totally determined by its temperature–salinity (T–S) profile (Su et al. 2016a). Accurate T–S data for the deglacial climate are scarce. CCSM3 offers currently one of the most advanced coupled GCM simulations for the T–S estimate: Through realistic changes in boundary conditions and forcing, it captures

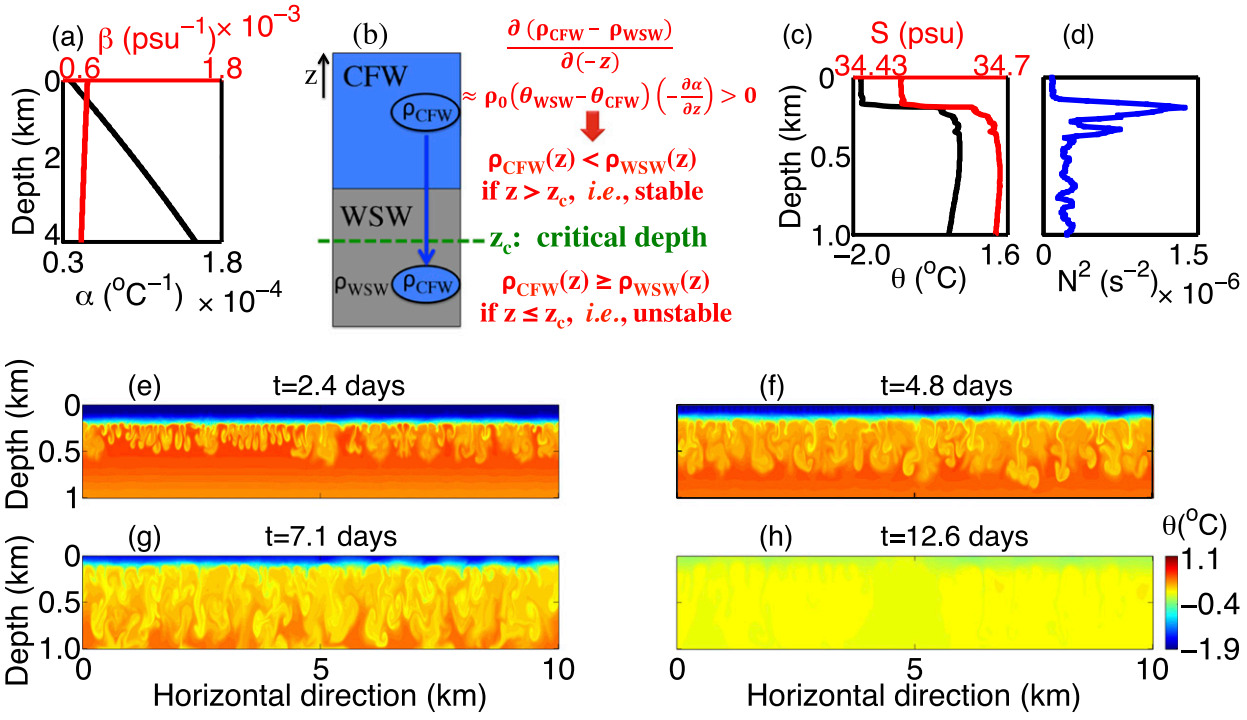

FIG. 2. (a) The vertical profile of thermal expansion coefficient $\alpha = -(1/\rho)(\partial\rho/\partial\theta)_{S,P}$ (black line) and saline contraction coefficient $\beta = (1/\rho)(\partial\rho/\partial S)_{\theta,P}$ (red line), where ρ is density, θ is potential temperature, S is salinity, and P is pressure. These are computed from constant profile of $\theta = -1$°C and $S = 34.0$ psu. OCAPE arises from thermobaricity: the strong dependency of α on depth. (b) Schematic illustration for the triggering of TCC and the release of OCAPE based on an idealized adiabatic argument. The θ and S of the adiabatically displaced CFW parcel does not change with depth. Also, $\partial\beta/\partial z$ is ≈ 0 from (a). Therefore, using the first-order Taylor series for density, one derives that $\rho_{\rm CFW} - \rho_{\rm WSW}$ increases with depth due to thermobaricity [$-\partial\alpha/\partial z > 0$, i.e., $\partial(\rho_{\rm CFW} - \rho_{\rm WSW})/\partial(-z) > 0$]. Thus there is a critical (threshold) depth z_c, above which the displaced CFW parcel remains lighter than the background WSW. If the CFW parcel is perturbed across z_c, it would be denser than the WSW and thus trigger the instability for TCC. The accumulation of OCAPE means the rise of the critical depth z_c, which weakens the threshold and makes it easier to be overcame (see also footnote 1). (c) Observed profiles of θ and S, obtained from the Weddell Sea (65.4605°N, 2.4007°E) on 2 Aug 1994, Antarctic Zone Flux Experiment (ANZFLUX) CTD station 48 (McPhee et al. 1996), and (d) their statically stable stratification is shown (i.e., positive buoyancy frequency N^2). This water column contains OCAPE of 1.1×10^{-3} J kg^{-1}, which is approximately ready to be released. (e)–(h) The snapshots in time of θ in our two-dimensional simulation of TCC initialized by the observed profiles of (c) in a 10-km horizontal domain. The model is nonhydrostatic and eddy-resolving in a rotating frame [essentially the same model of Akitomo et al. (1995) and Akitomo (2006)]. Triggered by the initial 4.2-day surface perturbations from realistic brine rejection (equivalent to 1 cm day^{-1} sea ice formation), the profile retains its statically stable stratification, but its OCAPE is then released into kinetic energy of TCC. The cabbeling effect further strengthens the TCC. Here 1 km is about the maximum depth of the convective overturning.

many major features of the deglacial climate evolution, including some T–S signals as inferred from observations (Liu et al. 2009; Shakun et al. 2012; Buizert et al. 2014). Diagnosing OCAPE in other GCMs would be our future work. (ii) Vertical mixing could partly dissipate OCAPE (Su et al. 2016b). CCSM3 parameterizes vertical mixing due to breaking internal waves and other processes (Collins et al. 2006). CCSM3 includes the mechanism for the diabatic dissipation of OCAPE and yet OCAPE is present. (iii) As introduced in section 1, observations indicate about 3°–5°C warming at intermediate depths of the North Atlantic during HS1 (Thiagarajan et al. 2014; Marcott et al. 2011; Alvarez-Solas et al. 2010). This induces CFW overlying WSW. Further, the North Atlantic should have a very weak stratification before the transition from HS1 to BA, because of either intermediate-depth warming or the potential surface buoyancy loss (e.g., a decrease of freshwater supply at surface) (Ganopolski and Rahmstorf 2001; Rasmussen and Thomsen 2004; Winton 1995). From Su et al. [2016a, Eqs. (16c) and (17c) therein], for weakly stratified quasi-two-layer oceans, the OCAPE is always positive and would increase following the warming of WSW.[1] Therefore, in principle, OCAPE would be built up due to the intermediate-depth (i.e.,

[1] Following section 4c of Su et al. (2016a) and the notations therein, the warming of WSW or the surface buoyancy loss induces a smaller $\Delta\rho$, which leads to a larger OCAPE and also a weaker threshold as represented by a higher z_S [see Eq. (12) therein, noting $\alpha_z < 0$].

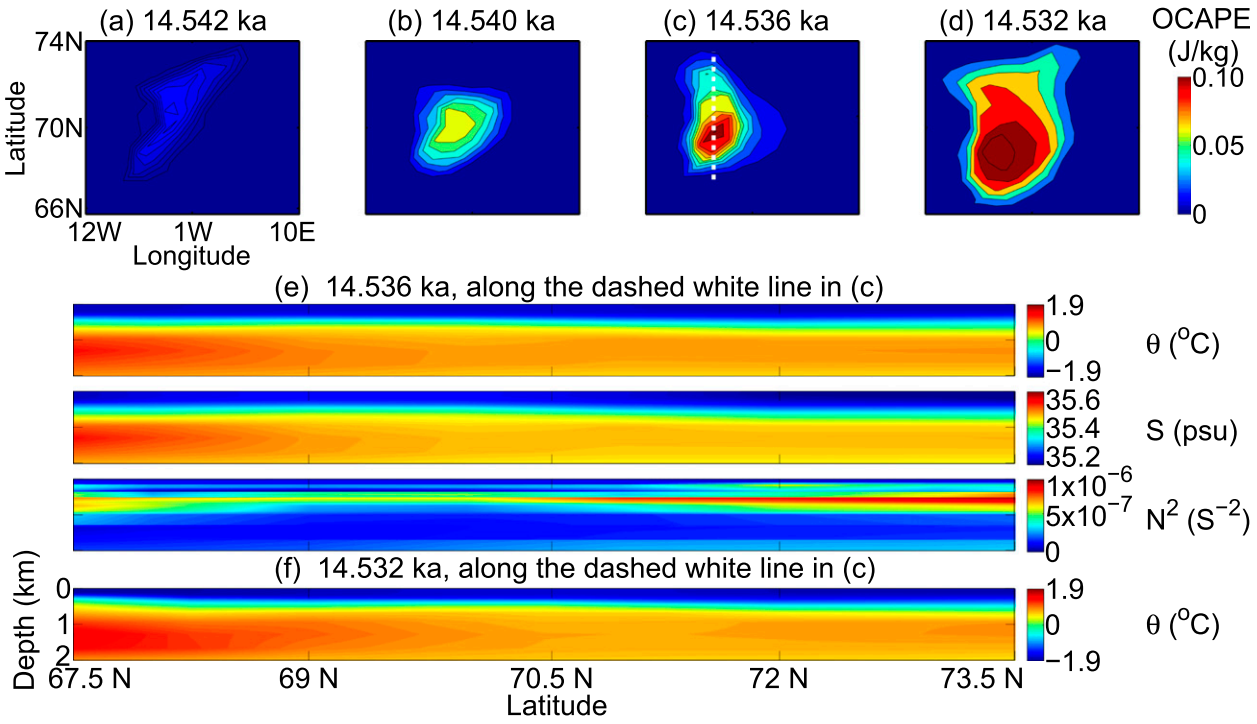

FIG. 3. (a)–(d) Decadal-scale accumulation of a basin-size (~700 km) OCAPE pattern in the North Atlantic at about the end of HS1, diagnosed using the monthly output (March data shown here) of the CCSM3 simulation of the last deglaciation (Liu et al. 2009; He et al. 2013). The OCAPE pattern starts to appear (a) about 14.542 ka and (b)–(d) grows in size and magnitude in the following decade. (e) As an example, the vertical section of θ, S, and N^2 for the dashed white line displayed in (c) (~6°W and 67.5°–73.5°N; 14.536 ka). This section has CFW overlying WSW, as required for OCAPE generation (see Fig. 2b). It has a statically stable stratification ($N^2 > 0$) despite of its large OCAPE. Because of this statically stable stratification, this section is not followed by obvious convection or vertical mixing in the CCSM3 simulation. (f) For example, even after four years (14.532 ka), the θ field still remains roughly unchanged in the CCSM3 simulation. (Contrast this lack of activity with our eddy-resolving simulation of TCC shown in Fig. 4.) Note that (a)–(d) share the same horizontal and vertical axis, and so do (e) and (f).

WSW) warming before the transition from HS1 to BA. We emphasize that the intermediate-depth warming alone (i.e., without surface freshwater forcing) in principle can induce the accumulation of OCAPE and the occurrence of TCC.

OCAPE keeps accumulating to a large magnitude while the water column remains in a statically stable stratification. This OCAPE accumulation continuously weakens the intrinsic threshold (see footnote 1) until the threshold is finally overshot, after which OCAPE is then released. Based on an idealized adiabatic argument, this intrinsic threshold is estimated by the energy barrier in a stable stratification that CFW parcels have to overcome to reach the critical depth within the WSW, where CFW parcels become equally dense as the surrounding WSW and thermobaricity allows them to accelerate downward and release OCAPE (Fig. 2b, see also the appendix). This estimate of threshold, however, should be treated only conceptually rather than quantitatively because real-ocean diabatic processes like cabbeling instability at the CFW–WSW interface would complicate this estimation (Harcourt 2005).

Although climate models like CCSM3 are capable of resolving the accumulation of OCAPE as shown above (Figs. 3a–d), it is difficult for them to account for the rapid release of OCAPE and thus TCC, for two reasons: 1) Current ocean GCMs have resolutions that are too coarse to resolve TCC, which has convective plumes with a typical horizontal scale of approximately 0.2–1 km [e.g., Figs. 2e–h; see also Akitomo et al. (1995) and Akitomo (2006)]. 2) The GCM convective parameterizations typically apply strong local diapycnal mixing in the vertical wherever the column is statically unstable (e.g., the K-profile parameterization; Large et al. 1994). This cannot account for the effect of TCC: the acceleration from thermobaricity produces vertical movement of CFW parcels to large depths (~1 km; e.g., Figs. 2f–h) without substantial mixing at intermediate depths. Therefore, in the CCSM3 simulation the hydrographic section shown in Fig. 3e is not followed by obvious convection (or strong vertical mixing) due to its statically stable stratification (e.g., Fig. 3e vs Fig. 3f, showing minimal changes of potential temperature even after four years). In contrast, we demonstrate in

section 3 that the hydrographic section shown in Fig. 3e is actually susceptible to TCC using a high-resolution eddy-resolving simulation (Fig. 4).

3. Simulated abrupt TCC events at the end of HS1

The decadal-scale OCAPE accumulation shown in Figs. 3a–d may induce TCC at the end of HS1, once the intrinsic threshold is overshot. Here we use a two-dimensional high-resolution simulation to investigate this possibility. The model and its numerical resolution are the same as the one mentioned in section 2 (for Figs. 2e–h). We have done simulations at finer resolutions, and they yield consistent results. A 2D model reduces the computational burden and generates a simulation of TCC consistent with a 3D model (Akitomo 2006; see section 4 for more discussion). Our simulation domain is a depth–latitude section located at around 6°W and 67.5°–73.5°N (white dashed line section shown in Fig. 3c, ~700 km horizontally). The bathymetry of this section is about 2–2.2 km deep and for convenience we set the domain bottom at a fixed 2-km depth.

For this section, numerous simulations are tested using various initializations from decadal-scale monthly outputs of CCSM3 that contain OCAPE (e.g., the ones shown in Figs. 3a–d). There are many examples in these hydrographic snapshots where TCC could occur, among which the earliest one is most relevant to real-ocean processes. Here we test various perturbation strengths: 50–200 W m^{-2} homogeneous surface cooling applied for the whole domain for the initial 1 day,[2] which also generates internal waves. These perturbations represent the regular strength of wintertime surface buoyancy forcing in the North Atlantic (Marshall and Schott 1999). We find that all OCAPE patterns earlier than March at 14.536 ka (e.g., Figs. 3a,b) cannot be released at all into kinetic energy in our test simulations. This is because for these snapshots, the prescribed perturbations are not strong enough to cross the threshold of thermobaric instability [section 4c of Su et al. (2016a)]. However, with the build-up of OCAPE due to intermediate-depth warming, the threshold becomes weaker until it is eventually crossed by the regular strength of perturbations. This is the threshold mechanism of why OCAPE can be accumulated to a large amount and suddenly triggered to be released into kinetic energy of TCC (Ingersoll 2005; Adkins et al. 2005).

The earliest snapshot from CCSM3 that is susceptible to thermobaric instability under our prescribed perturbations is from March at 14.536 ka, which initially has a statically stable stratification (Fig. 3e). Therefore, the triggered TCC is not based on the established convective-threshold mechanism, which requires a static instability (i.e., $N^2 < 0$; see also footnote 2). Here TCC could be triggered in our simulation by a surface cooling perturbation that is stronger than approximately 70 W m^{-2} (applied for the whole domain for the initial 1 day), which characterizes the magnitude of threshold for thermobaric instability for this snapshot of ocean. Further, the triggered TCC and the impact are essentially independent of the initial trigger as long as the direct contribution of the perturbation to kinetic energy is small (Su et al. 2016b). In contrast, the snapshot 1 month earlier (i.e., February at 14.536 ka from CCSM3) requires a domain-wide 1-day surface cooling larger than approximately 800 W m^{-2} for the triggering of TCC. This contrast of the required perturbations (800 vs 70 W m^{-2}) is mainly because that from February to March the North Atlantic experiences strong surface buoyancy loss in the GCM, which weakens the stratification and reduces the threshold for thermobaric instability (see also footnote 1; again the intermediate-depth warming alone could similarly reduce the threshold to this point, but it would take a longer time). Once triggered, both snapshots of ocean have been similarly overturned by TCC for the whole domain within a month. Here we focus on the simulation initialized by the snapshot of March at 14.536 ka, as detailed below.

The associated simulation of TCC is visualized in Fig. 4 (for the whole domain, ~700 km wide) and Fig. 5 (for a local zooming, ~40 km wide). After only about 0.6 days of surface cooling of 100 W m^{-2}, the perturbed CFW plumes sink into the WSW at two separate locations (~69.8° and 70.8°N) nearly simultaneously (Figs. 4b and 5b; see schematic in Fig. 2b). These two locations have about the maximal initial OCAPE in the whole domain (Fig. 3c) and are most susceptible to TCC. These initial convective plumes generate strong internal waves that spread the initial huge local convective perturbations (~2 km vertically) northward and southward, which are much stronger perturbations than normal background internal waves. These trigger other TCC events quickly along the way for the whole domain (Figs. 4c–e and 5c,d).

These TCC events have convective plumes with horizontal scales of approximately 0.2–1 km and large vertical velocities of approximately 8–15 cm s^{-1}. They only occur within the region that initially contains OCAPE, because TCC is powered by the release of OCAPE into kinetic energy with further intensification from the

[2] This magnitude of cooling changes the ocean stratification by only a small amount. As a scaling, consider 100 W m^{-2} cooling applies to the top 100 m of water (turbulent mixed layer) for 1 day. Then this water is cooled by (100 W m^{-2} × 1 day × 1 m^2)/(4200 J kg^{-1} °C^{-1} × 10^3 kg m^{-3} × 100 m × 1 m^2) ~0.02°C, which is much smaller than typical sea surface cooling from a big hurricane system ~1°C.

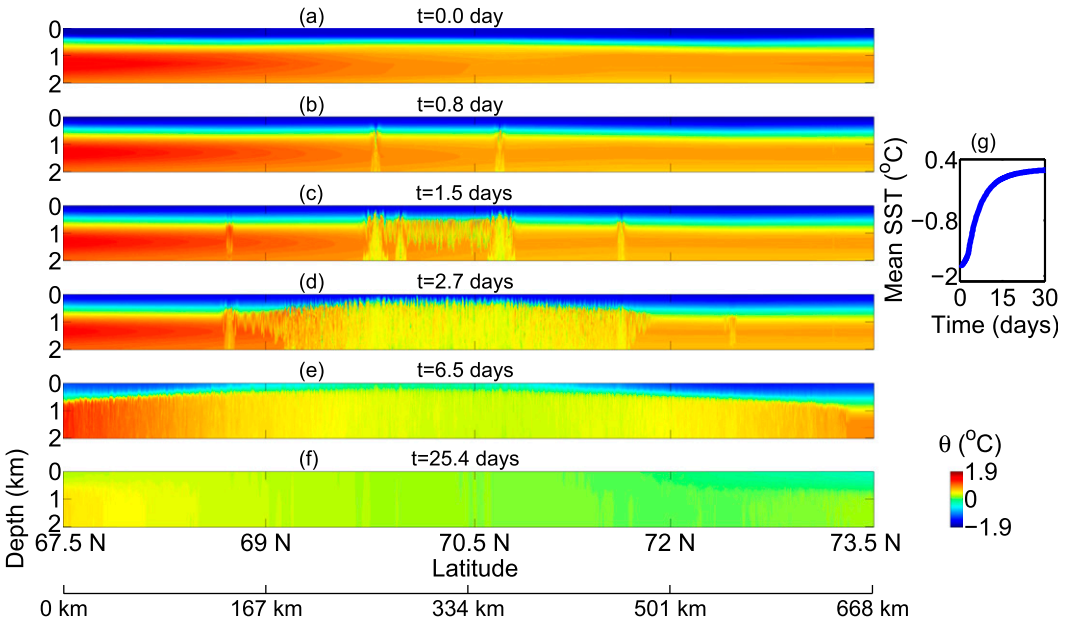

FIG. 4. (a)–(f) Snapshots in time of the θ field in our eddy-resolving two-dimensional simulation of TCC events in North Atlantic at about the end of HS1 (~6°W and 67.5°–73.5°N; 14.536 ka). The model is nonhydrostatic and eddy-resolving in a rotating frame [essentially the same model of Akitomo et al. (1995) and Akitomo (2006)], using the full equation of state of seawater (Jackett et al. 2006). We apply a vertical resolution of 10 m and a horizontal resolution of 50 m, which allow the resolving of TCC (Akitomo 2006; Harcourt 2005). The simulation is initialized by the θ and S snapshot output from CCSM3 simulation shown in Fig. 3e. This is the earliest monthly snapshot output that contains OCAPE (e.g., among Figs. 3a–d and many others) and is also susceptible to TCC in our simulations. Before that, this region is not susceptible to TCC. The domain size is approximately 700-km horizontal and 2-km vertical, with a sponge layer on the sides (not shown). TCC is triggered by a 1-day perturbation from inhomogeneous surface cooling of approximately 100 W m^{-2}. Because of the release of OCAPE, TCC starts at about t = 0.6–0.8 day simultaneously at two locations as shown in (b). The convective plumes have a horizontal size of approximately 0.2–1 km and spread quickly northward and southward by internal wave perturbations as shown in (c)–(f). Within a month, this basin-scale North Atlantic region (~700 km) has been thoroughly mixed by TCC events as shown in (f), which increases the sea surface temperature (SST) abruptly by about 2°C as shown in (g). [See Fig. 5 for the detail of convective plumes and its lateral spreading (by zooming into an approximate 40-km horizontal local domain).]

cabbeling effect. TCC causes strong local (~1-km depth) turbulent stirring, which vertically mixes the local water column within about 8 days (Fig. 5f). For the entire basin (~700-km scale), these TCC events cause a thorough vertical mixing (Fig. 4f) and thus increases the domain-averaged sea surface temperature by around 2°C within a month (Fig. 4g). This dramatic surface warming in North Atlantic exposes a huge basin-scale heat reservoir to the atmosphere and thus may directly contribute to the abrupt BA warming. These TCC events may further contribute to the BA warming by strengthening the AMOC, which causes more northward heat transport by decadal time scales (e.g., Banderas et al. 2012; Hogg et al. 2013; Buizert et al. 2014).

We also test simulation with the same configuration as above but excluding thermobaricity in the equation of state [the equation of state here follows Eq. (17) of Su et al. (2016b): the vertical profile of thermal expansion coefficient $\alpha(z)$ should be replaced by a constant $\alpha(z$ = 500 m), i.e., the value of α at the CFW–WSW interface at ~500-m depth in this scenario]. In this scenario the convection does not occur. This is because our mechanism relies on OCAPE to power the convection, while OCAPE is zero if excluding thermobaricity [see Eqs. (16c) and (17c) of Su et al. 2016a]. In contrast to a nonthermobaric convection event (i.e., by static instability), thermobaric instability supports deep penetrative convection that alters water properties to typically greater depths (~2 km), occurs by a more abrupt time scale (~days), and spreads horizontally in the OCAPE region.

4. Implications and further work

Our proposed convective threshold is provided by a quasi-two-layer structure (CFW overlying WSW; Fig. 4a) and thermobaricity, which permits decadal-scale

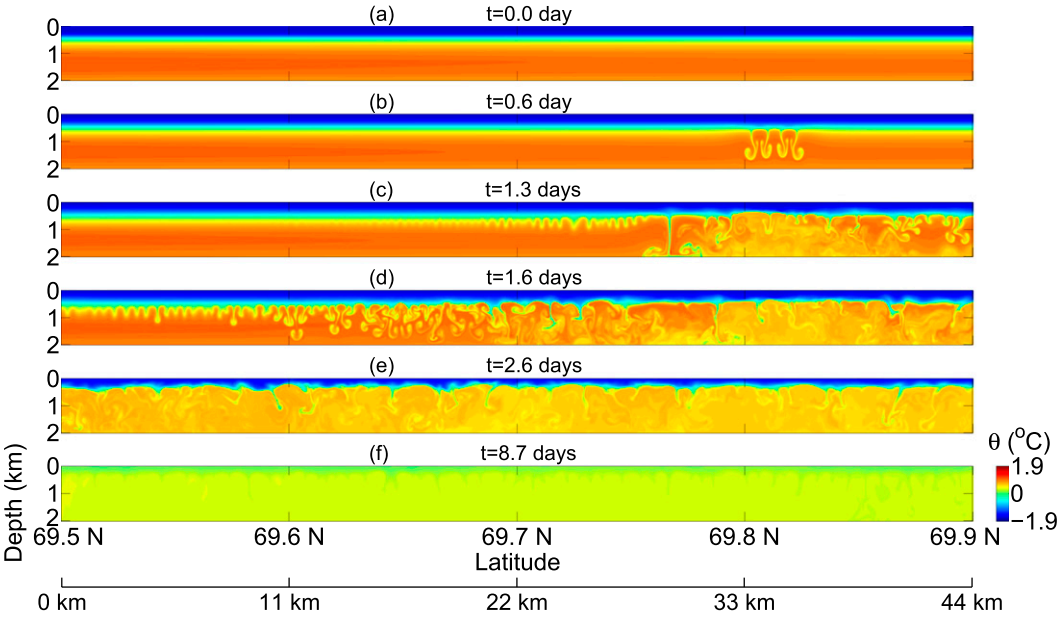

FIG. 5. (a)–(f) As in Figs. 4a–f, but zooming into an approximate 40-km horizontal local domain where TCC first appears. The convective plumes have a horizontal size of approximately 0.2–1 km. They first appear at $t = 0.6$ day as shown in (b) and the consequent perturbations spread laterally and quickly by internal waves. These trigger further TCC events southward and northward as in (c)–(e). Within 10 days, this approximate 40-km domain has been thoroughly mixed by TCC events.

accumulation of OCAPE to a large amplitude. This accumulation process weakens and finally overshoots the threshold, which releases OCAPE abruptly into kinetic energy to minimize the system's potential energy (Reddy 2002).

An advantage of our modified convective-threshold mechanism for the BA warming is that the time scale of basin-size sea surface warming by TCC events is only about one month, which is much shorter than the years to hundreds of years' time scales of regular buoyancy-driven convection events from the established convective-threshold mechanism (Ganopolski and Rahmstorf 2001; see also Buizert et al. 2014; Clark et al. 2002). This is consistent with previous studies that TCC typically occurs in a much shorter time scale than regular convection (Akitomo 1999; Denbo and Skyllingstad 1996). Thus the time scale of our result is helpful to explain the abrupt transition from one to three years of observed from the Greenland during the BA warming (Steffensen et al. 2008). However, the difference between the modified and the established convective-threshold mechanisms may not be easily reflected from the paleo observations due to their relatively low temporal and/or spatial resolutions (e.g., Thiagarajan et al. 2014). Further, our TCC mechanism is likely to mix the ocean to deeper depths in a single convection event (Denbo and Skyllingstad 1996), but it is possible that after years or decades the final overturning state at the end of the BA warming is the same. Finally, TCC can be an intrinsic/self-consistent component in the climate system. This is because TCC relies on the accumulation of OCAPE by the intermediate-depth warming, as a response to the heat/salt transport of the global ocean circulation. This is in a strong contrast to the simple-minded configuration of an essentially arbitrary surface freshwater forcing that controls the convection, which is used in numerous studies.

As far as we know, our study provides a first simulation to explore the potential importance of thermobaric instability for the abrupt paleoclimate changes. Our current simulation is idealized and should be treated with caveats. (i) Our model does not (and is difficult to) include the sea ice cover. Martinson (1990) and McPhee (2003) demonstrate the principal role of sea ice in maintaining the ocean column's stability. During convection the warm water brought to the surface would melt the sea ice and thus restratify the ocean column. This may offer a strong negative feedback on TCC. McPhee (2000, 2003) illustrates that thermobaric instability may still overcome this sea ice-induced barrier in the modern Weddell Sea. Harcourt (2005) simulates the fact that TCC may fully melt the sea ice cover (see his Fig. 19c). These studies provide important insights to explain the Weddell Polynya of the 1970s, which should be compared to the sea ice melting during the Bølling–Allerød warming. (ii) Sea ice and surface heat fluxes cool the warm water brought to the surface during

convection, which provides a destabilizing mechanism. As a test simulation, we restore the SST to the initial SST with a short relaxation time scale from 10 days to 1 month. This effect strengthens the TCC by only a small amount, since TCC has a short dynamic time scale (~days; Figs. 4b–d). In general, the "mixed boundary condition" (e.g., restoring SST and the differential surface salinity flux) is important to modulate the stability of the thermohaline circulations especially over a time scale of decades or longer (Yin 1995; Cai 1996; Mikolajewicz and Maier-Reimer 1994).

More questions need to be investigated in subsequent studies. (i) Millennial-scale geothermal heating during HS1, which is not included in this study and in most climate models, may likely cause significant warming at ocean depths (Adkins et al. 2005). Thus it may contribute to a larger OCAPE pattern compared to this study. (ii) Appropriate GCM convection parameterizations for TCC need to be developed such that TCC effects can be included in climate models. (iii) TCC is unlikely to be the only mechanism responsible for the whole BA warming. It is necessary to investigate the potential coupling effects between TCC and other important AMOC-related feedback mechanisms including ice sheets (e.g., Zhu et al. 2014), sea ice (e.g., the "sea ice switch" mechanism; see Gildor et al. 2014; Gildor and Tziperman 2003; Ashkenazy et al. 2013), atmospheric circulation (e.g., Banderas et al. 2012), the greenhouse effect (e.g., Zhang et al. 2014), and salt feedback (e.g., Knorr and Lohmann 2007). (iv) Our two-dimensional simulation does not resolve baroclinic instability, which may trigger TCC (Killworth 1979). It may also occur shortly after TCC at density fronts formed between the TCC-induced overturned regions and unoverturned regions (Akitomo 2006; from a 3D simulation). By comparing a 3D simulation to a 2D simulation, Akitomo (2006) finds that baroclinic instability produces additional upward heat transport (other than that from TCC) and does not qualitatively change the impacts of TCC. Thus, including baroclinic instability and using a 3D simulation may not qualitatively influence our conclusions.

Acknowledgments. We thank Stefan Rahmstorf and three anonymous reviewers for insightful comments on the manuscript. We also thank editor Anthony Broccoli for the constructive suggestions. We thank Jess Adkins and Andy Thompson for helpful comments on the initial manuscript. This material is based upon work supported by the National Science Foundation under Grant AST-1109299. F.H. was supported by the U.S. NSF (AGS-1203430) and by the NOAA Climate and Global Change Postdoctoral Fellowship program, administered by the University Corporation for Atmospheric Research. This research used resources of the Oak Ridge Leadership Computing Facility at the Oak Ridge National Laboratory, which is supported by the Office of Science of the U.S. Department of Energy under Contract DE-AC05-00OR22725.

APPENDIX

Mechanism for the Release of OCAPE to Kinetic Energy

We schematically illustrate the release of OCAPE to kinetic energy based on idealized assumptions. More details can be found in Su et al. (2016a,b). Thermobaricity is the significant increase of the thermal expansion coefficient α with the depth $-z$. In contrast, the saline contraction coefficient β is approximately constant with depth (Fig. 2a). We use the first-order Taylor series of density with respect to potential temperature θ and salinity S [Eq. (29) of Ingersoll 2005]:

$$\rho = \rho_0[1 - \alpha(\theta - \theta_0) + \beta(S - S_0)], \tag{A1}$$

where (ρ_0, θ_0, S_0) is the basic state for Taylor expansion. For two-layer profiles, we consider perturbations (e.g., breaking of internal waves or small changes in the buoyancy of the surface ocean) that move CFW parcels downward into WSW (Fig. 2b). The density difference between the perturbed CFW parcels and the background WSW is

$$\rho_{\mathrm{CFW}} - \rho_{\mathrm{WSW}} = \rho_0[-\alpha(\theta_{\mathrm{CFW}} - \theta_{\mathrm{WSW}}) + \beta(S_{\mathrm{CFW}} - S_{\mathrm{WSW}})]. \tag{A2}$$

Ideally, if assuming this process is adiabatic, both $\theta_{\mathrm{CFW}} - \theta_{\mathrm{WSW}}$ and $S_{\mathrm{CFW}} - S_{\mathrm{WSW}}$ would be constant with the depth $-z$. Noting that β is approximately constant with depth, we derive from (A2) that $\rho_{\mathrm{CFW}} - \rho_{\mathrm{WSW}}$ would increase with the depth $-z$ following

$$\frac{\partial(\rho_{\mathrm{CFW}} - \rho_{\mathrm{WSW}})}{\partial(-z)} = \rho_0(\theta_{\mathrm{WSW}} - \theta_{\mathrm{CFW}})\left(-\frac{\partial\alpha}{\partial z}\right) > 0. \tag{A3}$$

Therefore for a stable stratification, the CFW parcels are less dense than the WSW ($\rho_{\mathrm{CFW}} - \rho_{\mathrm{WSW}} < 0$) at the CFW–WSW interface. But if the CFW parcels are perturbed downward and eventually cross a certain critical depth (z_c in Fig. 2b), they would become negatively buoyant ($\rho_{\mathrm{CFW}} - \rho_{\mathrm{WSW}} > 0$) due to thermobaricity $-\partial\alpha/\partial z$ from (A3) (Fig. 2b). This releases OCAPE into kinetic energy and thus triggers TCC. The above offers a zero-order picture for the mechanism of TCC. In reality TCC is strongly modulated by diabatic processes [detailed in Su et al. (2016b)], with further intensification

from the cabbeling effect [for cabbeling, see McDougall (1987)].

REFERENCES

Adkins, J. F., A. P. Ingersoll, and C. Pasquero, 2005: Rapid climate change and conditional instability of the glacial deep ocean from the thermobaric effect and geothermal heating. *Quat. Sci. Rev.*, **24**, 581–594, doi:10.1016/j.quascirev.2004.11.005.

Akitomo, K., 1999: Open-ocean deep convection due to thermobaricity: 2. Numerical experiments. *J. Geophys. Res.*, **104**, 5235–5249, doi:10.1029/1998JC900062.

——, 2006: Thermobaric deep convection, baroclinic instability, and their roles in vertical heat transport around Maud Rise in the Weddell Sea. *J. Geophys. Res.*, **111**, C09027, doi:10.1029/2005JC003284.

——, T. Awaji, and N. Imasato, 1995: Open-ocean deep convection in the Weddell Sea: Two-dimensional numerical experiments with a nonhydrostatic model. *Deep-Sea Res. I*, **42**, 53–73, doi:10.1016/0967-0637(94)00035-Q.

Alley, R. B., 2007: Wally was right: Predictive ability of the North Atlantic "conveyor belt" hypothesis for abrupt climate change. *Annu. Rev. Earth Planet. Sci.*, **35**, 241–272, doi:10.1146/annurev.earth.35.081006.131524.

Alvarez-Solas, J., S. Charbit, C. Ritz, D. Paillard, G. Ramstein, and C. Dumas, 2010: Links between ocean temperature and iceberg discharge during Heinrich events. *Nat. Geosci.*, **3**, 122–126, doi:10.1038/ngeo752.

Arzel, O., A. Colin de Verdière, and M. H. England, 2010: The role of oceanic heat transport and wind stress forcing in abrupt millennial-scale climate transitions. *J. Climate*, **23**, 2233–2256, doi:10.1175/2009JCLI3227.1.

Ashkenazy, Y., M. Losch, H. Gildor, D. Mirzayof, and E. Tziperman, 2013: Multiple sea-ice states and abrupt MOC transitions in a general circulation ocean model. *Climate Dyn.*, **40**, 1803–1817, doi:10.1007/s00382-012-1546-2.

Banderas, R., J. Álvarez-Solas, and M. Montoya, 2012: Role of CO_2 and Southern Ocean winds in glacial abrupt climate change. *Climate Past*, **8**, 1011–1021, doi:10.5194/cp-8-1011-2012.

Brady, E. C., and B. L. Otto-Bliesner, 2011: The role of meltwater-induced subsurface ocean warming in regulating the Atlantic meridional overturning in glacial climate simulations. *Climate Dyn.*, **37**, 1517–1532, doi:10.1007/s00382-010-0925-9.

Broecker, W. S., 1994: Massive iceberg discharges as triggers for global climate change. *Nature*, **372**, 421–424, doi:10.1038/372421a0.

——, D. M. Peteet, and D. Rind, 1985: Does the ocean–atmosphere system have more than one stable mode of operation? *Nature*, **315**, 21–26, doi:10.1038/315021a0.

——, G. Bond, M. Klas, G. Bonani, and W. Wolfli, 1990: A salt oscillator in the glacial Atlantic? 1. The concept. *Paleoceanography*, **5**, 469–477, doi:10.1029/PA005i004p00469.

Buizert, C., and Coauthors, 2014: Greenland temperature response to climate forcing during the last deglaciation. *Science*, **345**, 1177–1180, doi:10.1126/science.1254961.

Cai, W., 1996: The stability of NADMF under mixed boundary conditions with an improved diagnosed freshwater flux. *J. Phys. Oceanogr.*, **26**, 1081–1087, doi:10.1175/1520-0485(1996)026<1081:TSONUM>2.0.CO;2.

Carlson, A. E., and P. U. Clark, 2012: Ice sheet sources of sea level rise and freshwater discharge during the last deglaciation. *Rev. Geophys.*, **50**, RG4007, doi:10.1029/2011RG000371.

Clark, P. U., N. G. Pisias, T. F. Stocker, and A. J. Weaver, 2002: The role of the thermohaline circulation in abrupt climate change. *Nature*, **415**, 863–869, doi:10.1038/415863a.

——, S. W. Hostetler, N. G. Pisias, A. Schmittner, and K. J. Meissner, 2007: Mechanisms for an 7-kyr climate and sea-level oscillation during marine isotope stage 3. *Ocean Circulation: Mechanisms and Impacts—Past and Future Changes of Meridional Overturning*, *Geophys. Monogr.*, Vol. 173, Amer. Geophys. Union, 209–246, doi:10.1029/173GM15.

Clement, A. C., and M. Cane, 1999: A role for the tropical Pacific coupled ocean–atmosphere system on Milankovitch and millennial timescales. Part I: A modeling study of tropical Pacific variability. *Mechanisms of Global Climate Change at Millennial Time Scales*, *Geophys. Monogr.*, Vol. 112, Amer. Geophys. Union, 363–372.

Collins, W. D., and Coauthors, 2006: The Community Climate System Model version 3 (CCSM3). *J. Climate*, **19**, 2122–2143, doi:10.1175/JCLI3761.1.

Denbo, D. W., and E. D. Skyllingstad, 1996: An ocean large-eddy simulation model with application to deep convection in the Greenland Sea. *J. Geophys. Res.*, **101**, 1095–1110, doi:10.1029/95JC02828.

Dokken, T. M., and E. Jansen, 1999: Rapid changes in the mechanism of ocean convection during the last glacial period. *Nature*, **401**, 458–461, doi:10.1038/46753.

Ganopolski, A., and S. Rahmstorf, 2001: Rapid changes of glacial climate simulated in a coupled climate model. *Nature*, **409**, 153–158, doi:10.1038/35051500.

——, and ——, 2002: Abrupt glacial climate changes due to stochastic resonance. *Phys. Rev. Lett.*, **88**, 038501, doi:10.1103/PhysRevLett.88.038501.

Gildor, H., and E. Tziperman, 2003: Sea-ice switches and abrupt climate change. *Philos. Trans. Roy. Soc. London*, **361A**, 1935–1944, doi:10.1098/rsta.2003.1244.

——, Y. Ashkenazy, E. Tziperman, and I. Lev, 2014: The role of sea ice in the temperature–precipitation feedback of glacial cycles. *Climate Dyn.*, **43**, 1001–1010, doi:10.1007/s00382-013-1990-7.

Harcourt, R. R., 2005: Thermobaric cabbeling over Maud Rise: Theory and large eddy simulation. *Prog. Oceanogr.*, **67**, 186–244, doi:10.1016/j.pocean.2004.12.001.

He, F., J. D. Shakun, P. U. Clark, A. E. Carlson, Z. Liu, B. L. Otto-Bliesner, and J. E. Kutzbach, 2013: Northern Hemisphere forcing of Southern Hemisphere climate during the last deglaciation. *Nature*, **494**, 81–85, doi:10.1038/nature11822.

Hemming, S. R., 2004: Heinrich events: Massive late Pleistocene detritus layers of the North Atlantic and their global climate imprint. *Rev. Geophys.*, **42**, RG1005, doi:10.1029/2003RG000128.

Hogg, A. M., H. A. Dijkstra, and J. A. Saenz, 2013: The energetics of a collapsing meridional overturning circulation. *J. Phys. Oceanogr.*, **43**, 1512–1524, doi:10.1175/JPO-D-12-0212.1.

Ingersoll, A. P., 2005: Boussinesq and anelastic approximations revisited: Potential energy release during thermobaric instability. *J. Phys. Oceanogr.*, **35**, 1359–1369, doi:10.1175/JPO2756.1.

Jackett, D. R., T. J. McDougall, R. Feistel, D. G. Wright, and S. M. Griffies, 2006: Algorithms for density, potential temperature, conservative temperature, and the freezing temperature of seawater. *J. Atmos. Oceanic Technol.*, **23**, 1709–1728, doi:10.1175/JTECH1946.1.

Killworth, P. D., 1979: On "chimney" formations in the ocean. *J. Phys. Oceanogr.*, **9**, 531–554, doi:10.1175/1520-0485(1979)009<0531:OFITO>2.0.CO;2.

Knorr, G., and G. Lohmann, 2007: Rapid transitions in the Atlantic thermohaline circulation triggered by global warming and meltwater during the last deglaciation. *Geochem. Geophys. Geosyst.*, **8**, Q12006, doi:10.1029/2007GC001604.

Knutti, R., J. Flückiger, T. Stocker, and A. Timmermann, 2004: Strong hemispheric coupling of glacial climate through freshwater discharge and ocean circulation. *Nature*, **430**, 851–856, doi:10.1038/nature02786.

Large, W. G., J. C. McWilliams, and S. C. Doney, 1994: Oceanic vertical mixing: A review and a model with a nonlocal boundary layer parameterization. *Rev. Geophys.*, **32**, 363–403, doi:10.1029/94RG01872.

Liu, Z., and Coauthors, 2009: Transient simulation of last deglaciation with a new mechanism for Bølling–Allerød warming. *Science*, **325**, 310–314, doi:10.1126/science.1171041.

Marcott, S. A., and Coauthors, 2011: Ice-shelf collapse from subsurface warming as a trigger for Heinrich events. *Proc. Natl. Acad. Sci. USA*, **108**, 13 415–13 419, doi:10.1073/pnas.1104772108.

Marshall, J., and F. Schott, 1999: Open-ocean convection: Observations, theory, and models. *Rev. Geophys.*, **37**, 1–64, doi:10.1029/98RG02739.

Martinson, D. G., 1990: Evolution of the Southern Ocean winter mixed layer and sea ice: Open ocean deepwater formation and ventilation. *J. Geophys. Res.*, **95**, 11 641–11 654, doi:10.1029/JC095iC07p11641.

McDougall, T. J., 1987: Thermobaricity, cabbeling, and water-mass conversion. *J. Geophys. Res.*, **92**, 5448–5464, doi:10.1029/JC092iC05p05448.

McManus, J., R. Francois, J.-M. Gherardi, L. Keigwin, and S. Brown-Leger, 2004: Collapse and rapid resumption of Atlantic meridional circulation linked to deglacial climate changes. *Nature*, **428**, 834–837, doi:10.1038/nature02494.

McPhee, M. G., 2000: Marginal thermobaric stability in the ice-covered upper ocean over Maud Rise. *J. Phys. Oceanogr.*, **30**, 2710–2722, doi:10.1175/1520-0485(2000)030<2710:MTSITI>2.0.CO;2.

——, 2003: Is thermobaricity a major factor in Southern Ocean ventilation? *Antarct. Sci.*, **15**, 153–160, doi:10.1017/S0954102003001159.

——, and Coauthors, 1996: The Antarctic Zone Flux Experiment. *Bull. Amer. Meteor. Soc.*, **77**, 1221–1232, doi:10.1175/1520-0477(1996)077<1221:TAZFE>2.0.CO;2.

Mignot, J., A. Ganopolski, and A. Levermann, 2007: Atlantic subsurface temperatures: Response to a shutdown of the overturning circulation and consequences for its recovery. *J. Climate*, **20**, 4884–4898, doi:10.1175/JCLI4280.1.

Mikolajewicz, U., and E. Maier-Reimer, 1994: Mixed boundary conditions in ocean general circulation models and their influence on the stability of the model's conveyor belt. *J. Geophys. Res.*, **99**, 22 633–22 644, doi:10.1029/94JC01989.

Rahmstorf, S., 1994: Rapid climate transitions in a coupled ocean–atmosphere model. *Nature*, **372**, 82–85, doi:10.1038/372082a0.

——, 1995a: Bifurcations of the Atlantic thermohaline circulation in response to changes in the hydrological cycle. *Nature*, **378**, 145–149, doi:10.1038/378145a0.

——, 1995b: Multiple convection patterns and thermohaline flow in an idealized OGCM. *J. Climate*, **8**, 3028–3039, doi:10.1175/1520-0442(1995)008<3028:MCPATF>2.0.CO;2.

——, 2001: A simple model of seasonal open ocean convection. Part I: Theory. *Ocean Dyn.*, **52**, 26–35, doi:10.1007/s10236-001-8174-4.

——, 2002: Ocean circulation and climate during the past 120,000 years. *Nature*, **419**, 207–214, doi:10.1038/nature01090.

Rasmussen, T. L., and E. Thomsen, 2004: The role of the North Atlantic Drift in the millennial timescale glacial climate fluctuations. *Palaeogeogr. Palaeoclimatol. Palaeoecol.*, **210**, 101–116, doi:10.1016/j.palaeo.2004.04.005.

——, D. W. Oppo, E. Thomsen, and S. J. Lehman, 2003: Deep sea records from the southeast Labrador Sea: Ocean circulation changes and ice-rafting events during the last 160,000 years. *Paleoceanography*, **18**, 1018, doi:10.1029/2001PA000736.

Reddy, J. N., 2002: *Energy Principles and Variational Methods in Applied Mechanics*. John Wiley & Sons, 592 pp.

Shaffer, G., S. M. Olsen, and C. J. Bjerrum, 2004: Ocean subsurface warming as a mechanism for coupling Dansgaard–Oeschger climate cycles and ice-rafting events. *Geophys. Res. Lett.*, **31**, L24202, doi:10.1029/2004GL020968.

Shakun, J. D., and Coauthors, 2012: Global warming preceded by increasing carbon dioxide concentrations during the last deglaciation. *Nature*, **484**, 49–54, doi:10.1038/nature10915.

Steffensen, J. P., and Coauthors, 2008: High-resolution Greenland ice core data show abrupt climate change happens in few years. *Science*, **321**, 680–684, doi:10.1126/science.1157707.

Stouffer, R. J., and Coauthors, 2006: Investigating the causes of the response of the thermohaline circulation to past and future climate changes. *J. Climate*, **19**, 1365–1387, doi:10.1175/JCLI3689.1.

Su, Z., A. L. Stewart, and A. F. Thompson, 2014: An idealized model of Weddell gyre export variability. *J. Phys. Oceanogr.*, **44**, 1671–1688, doi:10.1175/JPO-D-13-0263.1.

——, A. P. Ingersoll, A. Stewart, and A. Thompson, 2016a: Ocean convective available potential energy. Part I: Concept and calculation. *J. Phys. Oceanogr.*, **46**, 1081–1096, doi:10.1175/JPO-D-14-0155.1.

——, ——, ——, and ——, 2016b: Ocean convective available potential energy. Part II: Energetics of thermobaric convection and thermobaric cabbeling. *J. Phys. Oceanogr.*, **46**, 1097–1115, doi:10.1175/JPO-D-14-0156.1.

Thiagarajan, N., A. V. Subhas, J. R. Southon, J. M. Eiler, and J. F. Adkins, 2014: Abrupt pre-Bølling–Allerød warming and circulation changes in the deep ocean. *Nature*, **511**, 75–78, doi:10.1038/nature13472.

Weaver, A. J., O. A. Saenko, P. U. Clark, and J. X. Mitrovica, 2003: Meltwater pulse 1A from Antarctica as a trigger of the Bølling–Allerød warm interval. *Science*, **299**, 1709–1713, doi:10.1126/science.1081002.

Winton, M., 1995: Energetics of deep-decoupling oscillations. *J. Phys. Oceanogr.*, **25**, 420–427, doi:10.1175/1520-0485(1995)025<0420:EODDO>2.0.CO;2.

——, and E. Sarachik, 1993: Thermohaline oscillations induced by strong steady salinity forcing of ocean general circulation models. *J. Phys. Oceanogr.*, **23**, 1389–1410, doi:10.1175/1520-0485(1993)023<1389:TOIBSS>2.0.CO;2.

Yin, F., 1995: A mechanistic model of ocean interdecadal thermohaline oscillations. *J. Phys. Oceanogr.*, **25**, 3239–3246, doi:10.1175/1520-0485(1995)025<3239:AMMOOI>2.0.CO;2.

Zhang, X., G. Lohmann, G. Knorr, and C. Purcell, 2014: Abrupt glacial climate shifts controlled by ice sheet changes. *Nature*, **512**, 290–294, doi:10.1038/nature13592.

Zhu, J., Z. Liu, X. Zhang, I. Eisenman, and W. Liu, 2014: Linear weakening of the AMOC in response to receding glacial ice sheets in CCSM3. *Geophys. Res. Lett.*, **41**, 6252–6258, doi:10.1002/2014GL060891.